Draft version February 16, 2017
Typeset using LaTeX **manuscript** style in AASTeX61

arXiv:1702.04647v1 [astro-ph.HE] 14 Feb 2017

STUDY OF PARALLEL SHOCK ACCELERATION, THE BEND-OVER ENERGY OF SPECTRUM OF CHARGED ENERGETIC PARTICLES

L.-H. Zhang,[1,2] G. Qin,[3,2] P. Sun,[4,2] and H.-N. Wang[1]

[1] *National Astronomical Observatories, Chinese Academy of Sciences; Key Laboratory of Solar Activity, Chinese Academy of Sciences*
[2] *State Key Laboratory of Space Weather, National Space Science Center, Chinese Academy of Sciences, Beijing 100190, China*
[3] *School of Science, Harbin Institute of Technology, Shenzhen, 518055, China*
[4] *Departments of Planetary Sciences and Astronomy, University of Arizona, Tucson, AZ 85721, USA*

ABSTRACT

Shock acceleration is considered one of the most important mechanisms of astrophysical energetic particles' acceleration. In this work, we calculate large amount of test charged particles' trajectories accurately in a parallel shock with magnetic turbulence. We investigate energetic particles' acceleration mechanisms by calculating particles' energy and flux evolution with time. From simulations we obtain double power-law energy spectra with the bend-over energy increasing as a function of time. With the mean accelerating time and averaged momentum change during each cycle of particles crossing of shock from diffusive shock acceleration model, a time differential equation for the maximum of shock accelerated energy E_{acc} can be approximately obtained following Drury. We assume the bend-over energy as E_{acc}. It is found that the model of the bend-over energy generally agrees with the simulations, and that the bend-over energy model with our non-linear diffusion theory, NLGCE-F, performs better than that with the classic quasi-linear theory, QLT.

Keywords: shock, particle acceleration, magnetic turbulence, double power-law

Corresponding author: G. Qin
qingang@hit.edu.cn

1. INTRODUCTION

The collisionless shock acceleration of energetic particles, which is considered one of the key problems to study the sources of the solar energetic particles (SEPs) and the galactic cosmic rays (GCRs), has been studied by many scholars in decades (e.g., Fermi 1949; Bell 1978; Jokipii 1982; Drury 1983; Decker 1988; Krülls and Achterberg 1994; Lee et al. 1996; Zank et al. 2000; Bell 2004; Sun et al. 2007; Florinski et al. 2008b; Li et al. 2012; Wang et al. 2012; Qin et al. 2013; Zuo et al. 2013; Qi et al. 2017).

Different theories have been developed to explain the shock acceleration processes. The first theory is the shock drift acceleration (SDA) (Jokipii 1982; Forman and Webb 1985; Lee et al. 1996; Shapiro and Üçer 2003; Guo et al. 2014), in which the energy increase ΔE satisfies

$$\Delta E = q\boldsymbol{E} \cdot \Delta \boldsymbol{x} \tag{1}$$

with non-zero background magnetic field perpendicular to shock normal, where $\Delta \boldsymbol{x}$ is the particle's displacement variance, and the drift electrostatic field in the shock frame $\boldsymbol{E}$ is written as

$$\boldsymbol{E} = -\boldsymbol{U} \times \boldsymbol{B}, \tag{2}$$

here $\boldsymbol{U}$ is the background bulk velocity. If it is assumed that the background bulk velocity $\boldsymbol{U}$ is parallel to the shock normal, the electrostatic field would lie in the shock plane. When a particle makes gyro-motion near the shock plane, part of its gyro-cycle is in upstream and the rest part is in downstream. The charged particle will undergo acceleration on one side and deceleration on the other while moving back and forth through the shock plane before leaving the shock due to the convection of the bulk plasma flow. However, the charged particle's net energy change during this process is an acceleration. In this scenario, if the particles initial energy and gyro-radius are both too small, it will leave the shock very quickly and completely stay in the downstream because of convection. Therefore, the SDA has an injection problem that it is not effective if particle's initial energy is lower than a threshold value.

The second theory is the diffusive shock acceleration (DSA), or the first-order Fermi acceleration (Fermi 1949; Bell 1978; Drury 1983; Forman and Webb 1985; Kirk and Schneidr 1989;

Malkov and Drury 2001; Amato and Blasi 2005, 2006). Drury (1983) showed that for each cycle of particles' crossing of the shock plane, the mean acceleration time Δt is

$$\Delta t = \frac{4}{v}\left(\frac{\kappa_1}{U_1} + \frac{\kappa_2}{U_2}\right), \tag{3}$$

and the average momentum change is

$$\begin{aligned}\langle \Delta p \rangle =& 2p \int_0^1 \frac{\mu(U_1 - U_2)}{v} 2\mu d\mu \\ =& \frac{4}{3}\frac{U_1 - U_2}{v} p,\end{aligned} \tag{4}$$

where κ and U represent the diffusion coefficient and background bulk velocity, respectively, the subscripts 1 and 2 indicate variables in upstream and downstream, respectively, and μ is the particle's pitch angle cosine. Note that 2μ in the first line of Equation (4) is the statistical weighting factor. In this mechanism, if there is non-zero background magnetic field parallel to the shock normal, a particle obtains energy during their reflecting between the upstream and downstream of a shock because of diffusion parallel to the background magnetic field. Generally, DSA is not considered to have the injection problem. It is shown that with DSA the index of the energy spectrum γ satisfies (Decker and Vlahos 1986)

$$\gamma = \frac{r+2}{2(r-1)}, \tag{5}$$

where r is the compression ratio across the shock.

The third theory is the stochastic shock acceleration (SSA) with the magnetic turbulence or the second-order Fermi acceleration (Krülls and Achterberg 1994; Virtanen and Vainio 2005). The driving force of the SSA is the stochastic electric field $\boldsymbol{E}_b = -\boldsymbol{U} \times \delta\boldsymbol{b}$, where $\delta\boldsymbol{b}$ is the turbulent magnetic field superimposed on the mean magnetic field $\boldsymbol{B}$.

With the great development of super computer's ability of computation, different numerical simulation methods are proposed to better understand the acceleration processes. Generally, energetic particles' transport and acceleration in heliosphere can be studied by analyzing large amount of trajectories of particles which are obtained by solving the Newton's equation of motion with EM fields. If the EM fields are assumed to model a shock, the particle trajectories method can be used to

study the shock acceleration (e.g., Decker and Vlahos 1986). It is known that numerical simulations with such method need lots of computation resource. If we are not interested in individual particle's movements, especially the details of gyro-motion, the Fokker-Planck transport equation of energetic particles can be used to describe the change of the distribution function (Parker 1965; Skilling 1971; Qin et al. 2004, 2006). To study the shock acceleration of energetic particles, Zuo et al. (2011, 2013) used the transport equation method, which is more computational effective. However, one has to assume the model of particle's diffusion that is not always established in reality.

Charged particles can be accelerated by a shock, on the other hand, shock accelerated particles would influence EM fields, especially, they would excite shock waves. Therefore, the particle acceleration and EM fields evolution have to be coupled. Hybrid simulation is a particle-in-cell-type model that treats electrons as a fluid without mass while treats ions kinetically (Winske and Omidi 1996). Here, in kinetic simulations Maxwell's equations are solved self-consistently with plasma density and currents which themselves are generated from plasma particles (Winske and Omidi 1996). With conditions specially set, hybrid codes can be used to study particles acceleration and shock evolution self-consistently (e.g., Giacalone 2004, 2005; Guo and Giacalone 2010; Sugiyama 2011). However, hybrid codes are more complicated and require more programming effort, and the simulations need extensive computation resources. In order to pay more attention to the shock acceleration of energetic particles with specific shock conditions, e.g., geometry, compression ratio, magnetic fields, shock speed, and magnetic turbulence models, with more statistics results but less resources needed, the test particle model, which does not include energetic particles' feedback to the EM fields, can be very useful.

The diffusion of energetic particles in magnetic turbulence is very important to study shock acceleration of energetic particles. Jokipii (1966) developed a classical quasi-linear theory (QLT) of energetic particles diffusion in a slab model of magnetic turbulence. Matthaeus et al. (2003) provided the Non-Linear Guiding Center (NLGC) theory for the perpendicular diffusion coefficient. Qin (2007) modified the NLGC theory for perpendicular diffusion to obtain a NonLinear PArallel (NLPA) diffusion theory. It was shown that the solution of the NLGC and NLPA simultaneously agreed with simulations

very well. Furthermore, Qin and Zhang (2014) fit the numerical results of the NLGC+NLPA model with polynomials, which is called NLGCE-F. With the model NLGCE-F, one can calculate parallel and perpendicular diffusion coefficients with much reduced calculations.

In SEP events the energy spectrum of energetic particles usually shows a double power law or a power law with an exponential range in higher energy. The bend-over energy, E_b, in such kind of spectra is often in the range of several to tens of MeV per nucleon. The double power law energy spectrum can be written as (Band et al. 1993; Zhao et al. 2016)

$$\frac{\mathrm{d}J}{\mathrm{d}E} = \begin{cases} f_0 E^{-\alpha} \exp\left[(\alpha-\beta)\, E/E_b\right], & E \le E_b \\ f_0 E^{-\beta} E_b^{(\beta-\alpha)} \exp\left(\alpha-\beta\right), & E \ge E_b \end{cases} \tag{6}$$

Here α and β are the power law indices for the lower and higher energy ranges, respectively. It is interesting to study the origin of the double power law of SEP spectra. Some researchers suggested that the double power law spectrum can be caused by the shock acceleration of energetic particles (e.g., Mewaldt et al. 2012; Mason et al. 2012), but others assumed that it could originate from energetic particles' transport in heliosphere (e.g., Li and Lee 2015; Zhao et al. 2016)

In this paper, we study the parallel shock acceleration of test particles by solving the Newton-Lorentz equation in the shock frame with pre-exist turbulent magnetic field. With large amount of trajectories of particles we get double power law with bend-over energy E_b. We study the time variation of E_b by comparing the simulation results with theoretical modling. In section 2, we show our simulation model. In section 3, we show the theoretical models of the bend-over energy. In section 4, we show the numerical results and the comparison with different models. In section 5, we show conclusions and discussions.

2. SIMULATION MODEL

Test particle's motion in shock front frame is controlled by the Newton-Lorentz equation

$$\frac{\mathrm{d}\boldsymbol{p}}{\mathrm{d}t} = q\left(\boldsymbol{E} + \boldsymbol{v}\times\boldsymbol{B}\right), \tag{7}$$

where $\boldsymbol{p}$, $\boldsymbol{v}$, and q are the particle's momentum, velocity, and electric charge, respectively, and $\boldsymbol{E}$ and $\boldsymbol{B}$ are the local electric field and magnetic field, respectively. From this equation, particle's trajectory can be obtained with numerical calculations.

We simplify the shock as an infinite plane shown in Figure 1 as the vertical thick line, $\mathbf{n}$ represents the shock's normal direction and is anti-parallel to the z axis. $\boldsymbol{U}_1$ and $\boldsymbol{U}_2$ are the upstream and downstream solar wind speed, respectively, which are both set to be parallel to the shock normal. $\boldsymbol{B}_{10}$ and $\boldsymbol{B}_{20}$ represent the mean magnetic fields in upstream and downstream of the shock, respectively. θ_1 and θ_2 indicate the shock normal angle relative to magnetic field in upstream and downstream, respectively. The irregular thin lines that change with respect to the averaged $\boldsymbol{B}$ represent the turbulence magnetic field $\delta\boldsymbol{b}$.

In this paper, we use a slab plus 2D model of static turbulent magnetic field (Matthaeus et al. 1990; Mace et al. 2000; Qin et al. 2002a,b), which is different from that in Decker and Vlahos (1986). In our work, magnetic field is written as

$$\boldsymbol{B}(x', y', z') = \boldsymbol{B}_0(z') + \delta\boldsymbol{b}(x', y', z'),$$

where a Cartesian coordinate system is adopted, and the z'-axis is set to be parallel to the mean magnetic field $\boldsymbol{B}_0$, and the turbulent magnetic fluctuations $\delta\boldsymbol{b}$ have two components, the slab and 2D ones,

$$\delta\boldsymbol{b}(x', y', z') = \delta\boldsymbol{b}_{slab}(z') + \delta\boldsymbol{b}_{2D}(x', y'), \tag{8}$$

here, both the slab and 2D components are perpendicular to $\boldsymbol{B}_0$.

We neglect the induced electric field $|\boldsymbol{e}_k| \approx V_A|\boldsymbol{b}_k|$ of the turbulent magnetic field $\boldsymbol{b}_k(z)$ in plasma frame because of the fact that $V_A \ll |\boldsymbol{v}|$. Therefore, there is no electric field in the plasma frame on each side of the shock plane, and in shock front frame the $\boldsymbol{E}$ is the convective electric field because of the plasma bulk speed. In our simulations, the turbulence has a Kolmogorov's spectrum with a power index $\nu = -5/3$ at high wave-number k for each component. Except that the shock compression ratio $r = 3.85$, the other background parameters are chosen as those in Decker and Vlahos (1986). In the upstream, the mean magnetic field is $B_{10} = 50$ G, and the bulk velocity is $U_1 = 3.3 \times 10^6$ m/s.

The correlation scale length of the slab component of the turbulent magnetic field is $\lambda_{slab} = 6.67 \times 10^{-9}$ AU $= 1.00 \times 10^3$ m. The turbulent magnetic field $\delta \boldsymbol{b}_{slab}(z')$ is created with FFT in a box with size $L_{z'} = 64\lambda_{slab}$ along the mean magnetic field $\boldsymbol{B}_0$ and number of grids $N_{z'} = 2^{22} = 4194304$. In addition, to be different from that in Decker and Vlahos (1986), we apply the 2D component magnetic turbulence, with correlation scale length of 2D component $\lambda_{2D} = 0.1\lambda_{slab}$, in a box with size $L_{x'} = L_{y'} = 10\lambda_{slab}$ and number of grids $N_{x'} = N_{y'} = 4096$. The energy ratio of the two components of turbulence is set to be $E_{slab} : E_{2D} = 1 : 4$. In the upstream, $\delta b_{10}^2/B_{10}^2 = 0.19$, while $\delta b_{20}^2/B_{20}^2 = 0.38$ in the downstream. In the downstream side, the bulk velocity U_2 and mean magnetic field $\boldsymbol{B}_{20}$ are obtained from the Rankine-Hugoniot relations. Since the average of turbulence magnetic field is zero and turbulence level is small, we do not consider the Rankine-Hugoniot relations for the magnetic turbulence fields in the downside of shock.

We adopt a numerical code developed by Sun et al. (2007) using an adjustable time-step 4th order Ronge-Kutta method with accuracy of 10^{-9}. 40,000 protons with initial energy in the shock front frame $E_0 = 30$ KeV and gyro-radius $r_g \approx 5$ m are injected with isotropic distribution in the upstream with a distance $d = 1.1r_g$ to the shock front. Particles' simulations are performed with total time $t_{total} = 6.6$ ms, but without space limitation.

3. THEORETICAL MODEL OF THE BEND-OVER ENERGY

It is interesting to study the evolution of the bend-over energy if we assume the SEPs are accelerated by a shock. With the DSA model (Drury 1983) for each cycle of particles' crossing of the shock plane, from Equations (3) for the mean acceleration time Δt and Equation (4) for the average momentum change one can get

$$\frac{\mathrm{d}p}{\mathrm{d}t} \approx \frac{\Delta p}{\Delta t} = \frac{1}{3}\left(U_1 - U_2\right)\left(\frac{\kappa_1}{U_1} + \frac{\kappa_2}{U_2}\right)^{-1} p. \tag{9}$$

From Equation (9), we can see that the acceleration rate of particles by shocks depends on diffusion coefficient κ_i, so one gets different models of shock acceleration rate with different diffusion models.

It can be assumed that diffusion coefficients κ_i can be written as

$$\kappa_i = \kappa_{Ri}\left(\frac{p}{p_{ref}}\right)^{\xi_i}, \tag{10}$$

where κ_{Ri} and ξ_i are constants, and $p_{ref} = 5.34 \times 10^{-19}$ kg $\cdot$ m/s is the momentum of a proton with rigidity $R = 1$ GV.

With the integration of Equation (9), one can get the formula for the momentum p_{acc} of accelerated particles

$$\left(\frac{p_{acc}}{p_{ref}}\right)^{\xi_1} + g\left(\frac{p_{acc}}{p_{ref}}\right)^{\xi_2} = \left(\frac{p_0}{p_{ref}}\right)^{\xi_1} + g\left(\frac{p_0}{p_{ref}}\right)^{\xi_2} + \frac{1}{3}\frac{U_1^2}{\kappa_{R1}}\xi_1(r-1)t, \tag{11}$$

where $g = \xi_1\kappa_{R2}r/\left(\xi_2\kappa_{R1}\right)$, p_0 is particle's initial momentum, and the corresponding energy E_{acc} is

$$E_{acc} = \sqrt{p_{acc}^2c^2 + E_p^2} - E_p, \tag{12}$$

where E_p is the static energy of a proton. The Equation (11) is an implicant, by numerically solving which the momentum p_{acc} of particles with shock acceleration for time t could be obtained. It is less possible for particles to be accelerated to energy higher than E_{acc}. Therefore, the energy spectrum of particles accelerated by a shock could be turned around at the energy higher than E_{acc}, thus we can define a bend-over energy E_b as a function of time t

$$E_b \equiv E_{acc} = \sqrt{p_{acc}^2c^2 + E_p^2} - E_p. \tag{13}$$

If $\xi_1 = \xi_2 \equiv \xi$, the Equation (11) could be solved directly as,

$$p_{acc} = p_{ref}\left[\left(\frac{p_0}{p_{ref}}\right)^{\xi} + \frac{U_1^2\xi}{3}\frac{r-1}{\kappa_{R1} + r\kappa_{R2}}t\right]^{1/\xi}. \tag{14}$$

Since we study parallel shock acceleration in this work, diffusion coefficients in Equation (10) are for parallel diffusion. For our new nonlinear diffusion theory (Qin and Zhang 2014, NLGCE-F theory), we firstly calculate a large amount of κ_i using the computer codes downloaded from the website http://www.qingang.org.cn/code/NLGCE-F with different proton momentum in parameters both up- and down-stream, then we numerically fit κ_i data with Equation (10) and get ξ_i and κ_{Ri} both in upstream ($i = 1$) and down-stream ($i = 2$). The fitting results are shown in Table 1. From the table we can see that $\xi_1 = \xi_2$ for NLGCE-F model from the numerical fitting in the conditions of this work. In addition, for the QLT theory, ξ_i and κ_{Ri} can be calculated analytically and shown in Table 1. One can find that for QLT $\xi_1 = \xi_2$. Therefore, the momentum of accelerated particles p_{acc} with

QLT and NLGCE-F theories can be calculated directly from Equation (14), and the corresponding bend-over energy, which are indicated by $E_b^{\rm QLT}$ and $E_b^{\rm NLGCE\text{-}F}$, respectively, could be obtained.

From Decker and Vlahos (1986), if charged particles are injected near the shock, after the shock acceleration for long enough time the energy spectrum becomes stable with power law index γ satisfying Equation (5). In this work, the compression ratio of the shock $r = 3.85$, then the theoretical power law index of the shock accelerated particles energy spectrum is $\gamma = 1.03$. It can be assumed that the power law index model from Equation (5) is for α in the energy range lower than the bend-over energy E_b.

4. NUMERICAL RESULTS AND COMPARISON WITH THEORIES

Figure 2 shows the trajectory of one of the test particles accelerated by a parallel shock with $\theta_1 = \theta_2 = 0$ as a function of time. The top one to three panels show the $x-$, $y-$, and $z-$ components, respectively, of the particle's position in unit of $\lambda = \lambda_{slab}$, the correlation scale length of slab turbulence. The fourth to sixth panels show the $x-$, $y-$, and $z-$ components, respectively, of the particle's momentum in unit of p_{ref}. The bottom panel indicates the energy of the particle in the unit of the particle's initial energy $E_0 = 30$ KeV. The vertical blue dashed lines indicate the time when the particle crosses the shock plane. The red lines in the top six panels show zero in vertical axis.

It is known that a particle will be accelerated and gain energy when it crosses the shock plane back and forth. From top three panels of Figure 2 we can see that in the time interval $0.9 \sim 3.1$ ms (noted as time interval A) the particle crosses the shock plane for many times, but at the time outside the time interval A the particle does not cross the shock, especially after the time interval A, the particle's $z-$ component of position increases persistently with time and it moves far away from the shock plane. In addition, from the 4th to 6th panels of Figure 2, one can find that the particle generally perform gyro-rotation in the $x - y$ plane, while it is scattered back and forth near the shock plane in z direction in the time interval A, and moves away from the shock plane after the time interval A. It can be seen that in the time interval A, the crests of p_x and p_y increase much more significantly than the crests of p_z, so it is shown that the energy gain is mainly in the

gyro-rotation plane during the shock crossings. However, after the time interval A, the crests of p_x and p_z do not increase anymore, but the magnitude of p_z increases to the similar level of p_x and p_z. It is assumed that the energy homogenization among different directions are due to the pitch angle diffusion by magnetic turbulence. From the bottom panel of Figure 2, the particle gains energy more than 700 times of its original energy. But at the time outside the time interval A, particle's energy keeps almost constant.

From the trajectories of test particle simulations, we calculate particles energy spectra with different time, $t_i = i\Delta t$, with i from 1 to 10 and $\Delta t = 0.66$ ms. In Figure 3, the colored solid lines with diamonds show the particles' energy spectra after the parallel shock acceleration for different time. For the simulation results from bottom to top, the time for simulation is increasing, however, the energy spectra from simulation results are multiplied by arbitrary factors for better view. Note that we do not show energy spectra with energy less than the initial energy E_0 since in reality the background spectrum below E_0 is dominant. In Figure 3 we can see, every energy spectrum can be divided into two power law energy ranges with different power indices, especially when particles are accelerated by the shock for a longer time. It also can be seen that the bend-over energy E_b, at which the spectra would change from one power law range to another, is increasing with the increase of the time of shock acceleration.

We would like to fit the power spectra from simulations with the double power law Equation 6, however, since we don't have spectrum in high energy range from simulations, for simplicity purpose, we ignore the exponential factor in Equation 6, so the double power law Equation 6 becomes

$$\frac{\mathrm{d}J}{\mathrm{d}E} = \begin{cases} f_0 E^{-\alpha}, & E \leq E_b \\ f_0 E^{-\beta} E_b^{(\beta-\alpha)}, & E \geq E_b \end{cases} \tag{15}$$

With different time of acceleration, we fit the power spectra from simulations with the double power law Equation (15) using the least square method in log-log space. In Figure 3, we show the fitted double power-law results with dotted black lines and the corresponding bend-over energy E_b with colored filled circles.

Furthermore, we show the fitted bend-over energy $E_b^{\rm sim}$ with filled circles as a function of acceleration time in Figure 4. Note that the error bars with $E_b - \Delta E_1$ and $E_b + \Delta E_2$ are obtained by modifying the fitted bend-over energy to a lower and higher values, $E_b - \Delta E_1$ and $E_b + \Delta E_2$, respectively, to make the least-square-values 10% higher than that with the best fitted ones E_b. In Figure 3 it is shown that as time increases, the bend-over energy also increases.

Beside the results from simulations, Figure 4 also shows the theoretical bend-over energy $E_b^{\rm NLGCE\text{-}F}$ (solid line) and $E_b^{\rm QLT}$ (dashed line) with the diffusion coefficient models NLGCE-F and QLT, respectively. In the figure, we find that both $E_b^{\rm NLGCE\text{-}F}$ and $E_b^{\rm QLT}$ follow the similar trend as $E_b^{\rm sim}$ does to increase as time, but $E_b^{\rm NLGCE\text{-}F}$ has a better performance than $E_b^{\rm QLT}$ to compare with simulations. In addition, with short time range, i.e., $t < 5$ ms, $E_b^{\rm sim}$ is larger than both $E_b^{\rm NLGCE\text{-}F}$ and $E_b^{\rm QLT}$, but with long time range, i.e., $t \gtrsim 5$ ms, $E_b^{\rm sim}$ agrees with $E_b^{\rm NLGCE\text{-}F}$ much better. Generally speaking, $E_b^{\rm NLGCE\text{-}F}$ fit to the simulation results $E_b^{\rm sim}$ for the parallel shock acceleration much better than $E_b^{\rm QLT}$.

Figure 5 shows the time evolution of the power law indices, α and β, of simulated particle spectra in lower and higher energy ranges with solid and dashed lines, respectively. The dotted line indicates the theoretical results γ from Equation (5) by Decker and Vlahos (1986). It is clear that the power law index of simulated particle spectrum in lower energy range α is larger than the theoretical model γ, but it generally agrees with γ. In addition, as time increases, α becomes smaller to get closer to γ. Furthermore, one can find that the power law index of simulated particle spectrum in higher energy range β is more than twice of γ, and β increases as time goes on.

5. CONCLUSION AND DISCUSSION

Hybrid codes are effective to study particles acceleration and shock evolution self-consistently. However, it is often interesting to study the shock acceleration of energetic particles with some predetermined shock conditions, e.g., geometry, compression ratio, magnetic fields, shock speed, and magnetic turbulence models, so it is useful to study shock acceleration by calculating test particles' trajectories. In addition, since test particle simulations need much less computation resources, it is possible for us to study particles acceleration with more statistics, in larger computation space and time. In this paper, we study parallel shock acceleration with numerical simulations of large amount

of test particles' trajectories by solving the Newton-Lorentz equation with magnetic turbulence. The shock is simplified to be without thickness. In addition, we set static magnetic turbulence superimposed on the static background magnetic field.

From our simulations it is found that charged particles can be accelerated to a very high energy level, some particles can even get energy gain of hundreds of times of their initial energy in milliseconds. Furthermore, the shock accelerated particles from simulations show a double power law spectrum. The power law index of the lower energy range approximately agrees with the power law index model by Decker and Vlahos (1986), but the power law index of the higher energy range is more than twice of the theoretical value by Decker and Vlahos (1986). It is also found that from simulations the bend-over energy, which is between the two energy ranges of the double power law spectrum, increases as time goes on.

With the mean acceleration time and the average momentum change during each cycle of particles' crossing of the shock (Drury 1983), we get the energy E_{acc} of shock accelerated particles as a function of time by the integration. In addition, we assume the bend-over energy is equal to E_{acc} since it is less possible for particles to be accelerated to energy higher than E_{acc} at any time. The theory of the bend-over energy depends on the diffusion model. We compare the bend-over energy from simulations with that from theoretical ones with QLT and NLGCE-F models, and we find that the theoretical results generally agree with simulation ones. In addition, The theory with NLGCE-F diffusion model performs better than that with QLT diffusion model. Furthermore, as time goes on the theory with NLGCE-F has better agreement with simulation results. This result is another way to show that the diffusion model of NLGCE-F is more accurate than that of QLT (Qin and Zhang 2014).

Our results from both numerical simulations and theoretical models show that the parallel shock could introduce double power-law of energy spectrum of charged particles, with the increasing of bend-over energy as time goes on. Beside the transport effects, shock acceleration provides another way to possibly explain the initiation of double power-law spectrum of SEPs in solar wind. In this work, because of the limit of computing resources, we do not simulate the shock acceleration for very long time, so that we do not obtain a power-law spectrum of energetic particles with the bend-over

energy as large as that observed in solar wind. In the future, we plan to study shock acceleration with much longer time so that we might be able to obtain more realistic double power-law spectrum of energetic particles.

We are partly supported by grants NNSFC 41125016, NNSFC 41374177, and NNSFC 41574172.

REFERENCES

Amato, E., & Blasi, P., 2005, MNRAS, 364, L76

Amato, E., & Blasi, P., 2006, MNRAS, 371, 1251

Band, D., Matteson, J., Ford, L., et al. 1993, ApJ, 413, 281

Bell, A. R., 1978, MNRAS, 182, 147

Bell, A. R., 2004, MNRAS, 353, 550

Decker, R. B., & Vlahos, L., 1986, ApJ, 306, 710

Decker, R. B., 1988, SSRv, 48, 195

Drury, L. OC., 1983, Rep. Prog. Phys., 46, 973

Fermi, E., 1949, Phys. Rev. 75, 1169

Florinski, V., Zank, G. P., & le Roux, J. A., 2008, Adv. Space Res., 41, 361

Florinski, V., 2009, SSRv, 143, 111

Forman, M. A., & Webb, G. M., 1985, in Collisionless Shocks in the Heliosphere: A Tutorial Review, Geophysical Monograph, Vol. 34, ed. R. G. Stone & B. T. Tsurutani (Washington, DC: American Geophysical Union), 91

Giacalone, J., 2004, ApJ, 609, 452

Giacalone, J., 2005, ApJ, 624, 765

Guo, F. & Giacalone, J., 2010, ApJ, 715, 406

Guo, X. Y., Sironi, L., & Narayan, R., 2014, ApJ, 794, 153

Jokipii, J. R., 1966, ApJ, 146, 480

Jokipii, J. R., 1982, ApJ, 255, 716

Kato, T. N., & Takabe, H., 2008, ApJ, 681, L93

Kirk, J. G., & Schneider, P., 1987, ApJ, 315, 425

Krülls, W. M., & Achterberg, A., 1994, A&A, 286, 314

le Roux, J. A., & Webb, G. M., 2009, ApJ, 693, 534

le Roux, J. A., Webb, G. M., Florinski, V., & Zank, G. P., 2007, ApJ, 662, 350

Lee, M. A., Shapiro, V. D., & Sagdeev, R. Z., 1996, J. Geophys. Res., 101, 4777

Li, G., & Lee, M. A., 2015, ApJ, 810, 82

Li, G., Shalchi, A., Ao, X., Zank, G., & Verkhoglyadova, O. P., 2012, J. Adv. Space Res., 49, 1067

Mace, R. L., Matthaeus, W. H., & Bieber, J. W., 2000, ApJ, 538, 192

Malkov, M. A., & Drury, L. O'C., 2001, Rep. Prog. Phys., 64, 429

Mason, G. M., Li, G., Cohen, C. M. S., Desai, M. I., Haggerty, D. K., Leske, R. A., Mewaldt, R. A., & Zank, G. P., 2012, ApJ, 761, 104

Matthaeus, W. H., Goldstein, M. L., & Roberts, D. A., 1990, J. Geophys. Res., 95, 20673

Matthaeus, W. H., Qin, G., Bieber, J. W., & Zank, G. P., 2003, ApJ, 590, L53

Mewaldt, R. A., Looper, M. D., Cohen, C. M. S., Haggerty, D. K., Labrador, A. W., Leske, R. A., Mason, G. M., Mazur, J. E., & von Rosenvinge, T. T., 2012, SSRv, 171, 97

Ohira, Y., Reville, B., Kirk, J. G., & Takahara, F., 2009, ApJ, 698, 445

Parker, E. N., 1965, Planet. Space Sci., 13, 9

Qi, S.-Y., Qin, G., & Wang, Y. 2017, Res. Astron. Astrophys., in press

Qin, G., Matthaeus, W. H., & Bieber, J. W., 2002, ApJ, 578, L117

Qin, G., Matthaeus, W. H., & Bieber, J. W., 2002, Geophys. Res. Lett., 29, 1048

Qin, G., Zhang, M., Dwyer, J.R., & Rassoul, H. K., 2004, ApJ, 609, 1076

Qin, G., Zhang, M., & Dwyer, J.R., 2006, J. Geophys. Res., 111, A08101

Qin, G., 2007, ApJ, 656, 217

Qin, G., Wang, Y., Zhang, M., & Dalla, S. 2013, ApJ, 766, 74

Qin, G., & Zhang, L. H., 2014, ApJ, 787, 12

Riquelme, M. A., & Spitkovsky, A., 2011, ApJ, 733, 63

Shapiro, V. D., & Üçer, D., 2003, Planet. Space Sci., 51, 665

Skilling, J., 1971, ApJ, 170, 265

Sugiyama, T., 2011, Phys. Plasmas, 18, 022302

Sun, P., Qin, G., & Wang, C., 2007, Chin. J. Space Sci., 27(6), 441

Treumann, R. A., 2009, A&A Rv, 17, 409

Virtanen, J. J. P., & Vainio, R., 2005, ApJ, 621, 313

Wang, Y., Qin, G., & Zhang, M. 2012, ApJ, 752, 37

Winske, D., & Omidi, N., 1996, J. Geophys. Res., 101, 17287

Zank, G. P., Rice, W. K. M., & Wu, C. C., 2000, J. Geophys. Res., 105, 25079

Zhang, M., 1999, ApJ, 513, 409

Zhang, M., 2000, ApJ, 541, 428

Zhao, L. L., Zhang, M., & Rassoul, H. K., 2016, ApJ, 821, 62

Zuo, P., Zhang, M., Gamayunov, K., Rassoul, H. K., & Luo, X., 2011, ApJ, 738, 168

Zuo, P., Zhang, M., & Rassoul, H. K., 2013, ApJ, 767, 6

Table 1. ξ_i and κ_{Ri} from NLGCE-F theory and QLT theory.

Theory	Parameter	Upstream	Downstream
NLGCE-F	ξ_i	1.28	1.28
	κ_{Ri} (m^2/s)	5.16×10^{12}	3.37×10^{12}
QLT	ξ_i	1.33	1.33
	κ_{Ri} (m^2/s)	1.26×10^{13}	6.30×10^{12}

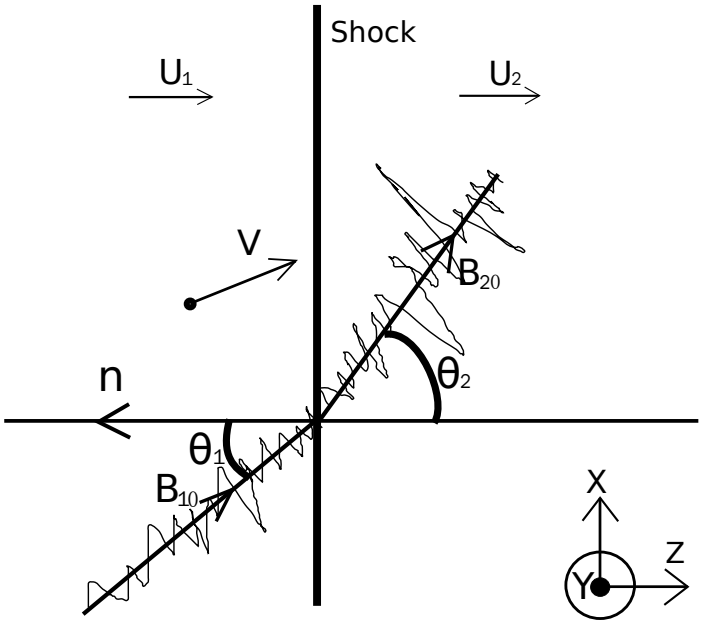

Figure 1. Pure plane shock model with vertical line indicating shock front. The horizontal line with $\boldsymbol{n}$ represents the shock normal direction. $\boldsymbol{B}_{10}$ and $\boldsymbol{B}_{20}$ indicate the averaged magnetic field in upstream and downstream, respectively, with the irregular thin lines that change with respect to the averaged $\boldsymbol{B}_0$ representing the turbulence magnetic field $\delta\boldsymbol{B}$. $\boldsymbol{U}_1$ and $\boldsymbol{U}_2$ indicate the velocity of the background plasma that is parallel to the shock normal in upstream and downstream, respectively. The Cartesian coordinate system is plotted in the bottom right.

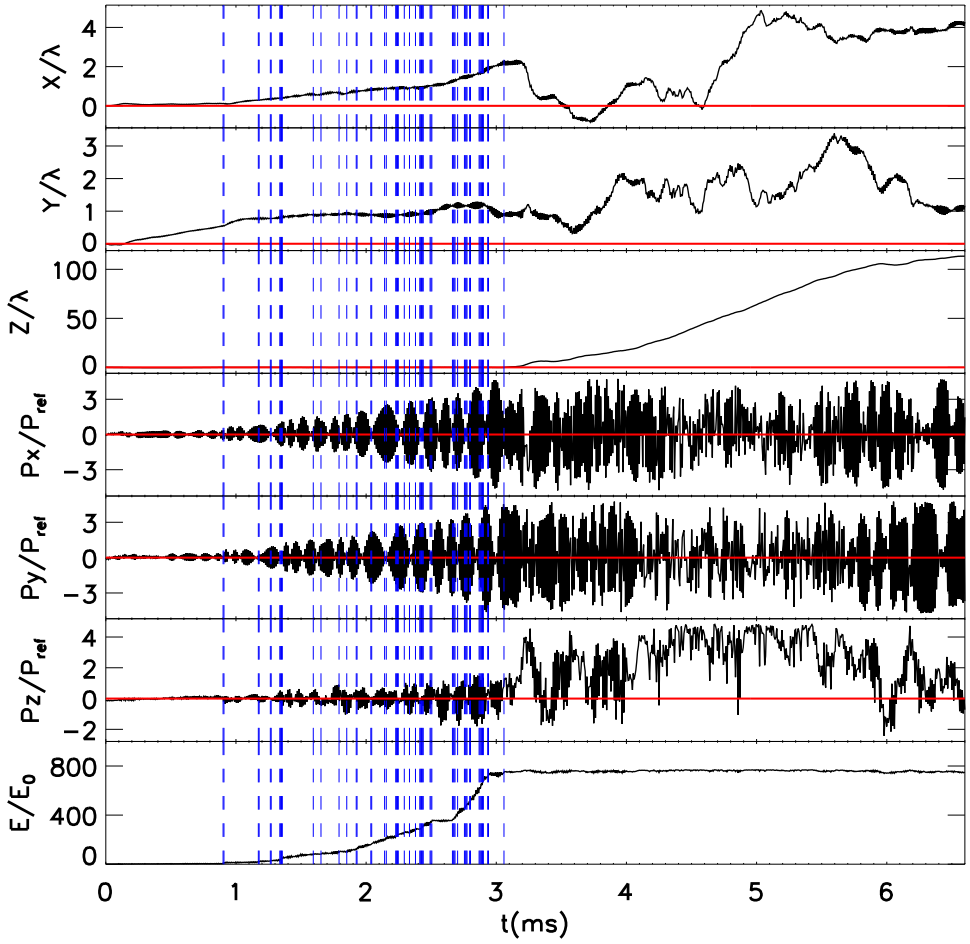

Figure 2. The trajectory of one of the test particles as a function of time. The top three panels show the particle's position in the Cartesian coordinate system, the fourth to sixth panels show the particle's momentum in each direction, and the bottom panel indicates the particle's energy. The vertical blue lines indicate the times when the particle crosses the shock plane. The red lines in the top six panels represent zero in vertical axis.

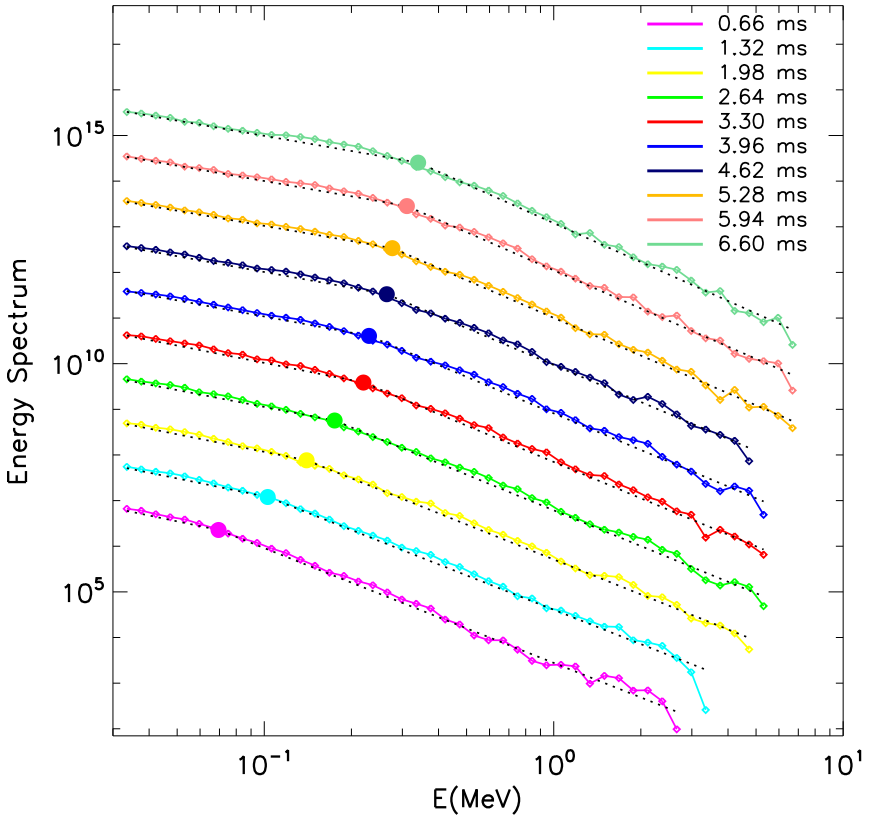

Figure 3. The energy spectra for shock accelerated particles. The solid colored lines are results from simulations for different acceleration time that are multiplied by arbitrary constants for good view. The dotted lines indicate the fitted energy spectra. The filled colored circles show the fitted bend over energy.

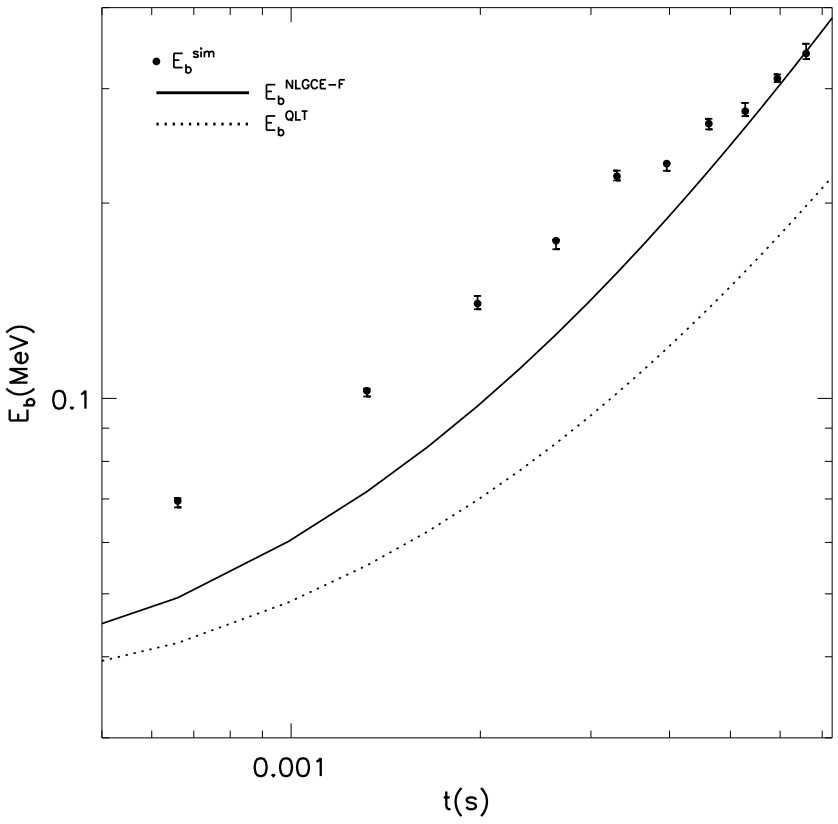

Figure 4. The bend-over energy as a function of time from simulations (diamonds), theory with NLGCE-F (solid line), and theory with QLT (dotted line).

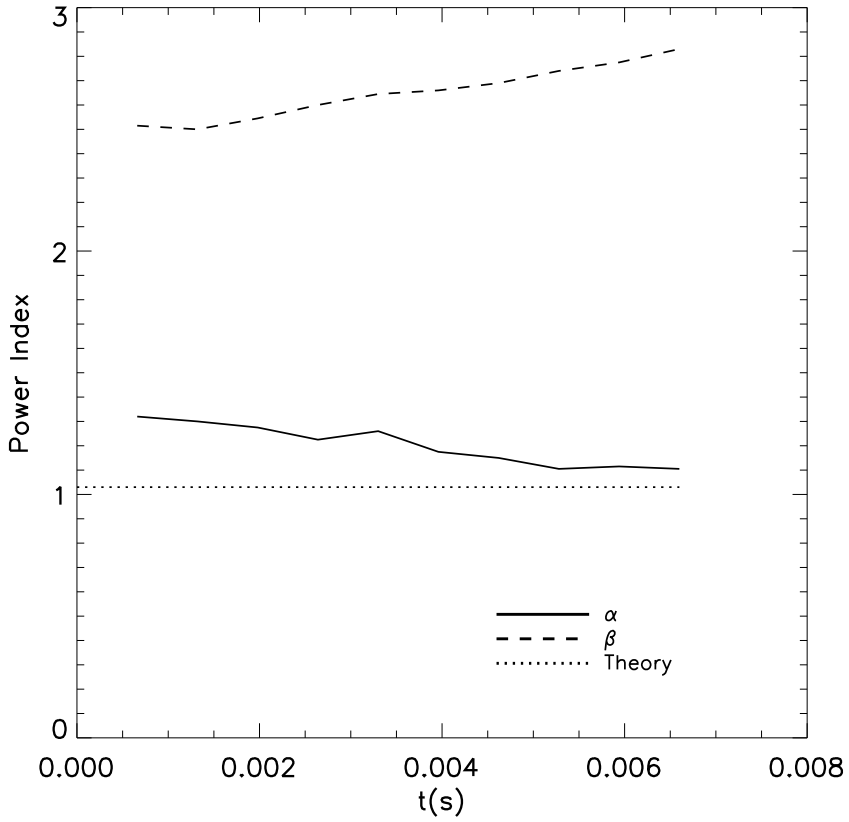

Figure 5. Power law index of spectrum of shock accelerated particles as a function of time. Solid and dashed lines indicate results from simulations for lower and higher energy range, α and β, respectively, and dotted line indicates the theoretical results.